

# Detrending GOLD FUV Data to Reveal Equatorial Plasma Bubble Structures

Rezy Pradipta<sup>1</sup>, Keith M. Groves<sup>1</sup>, and Chaosong Huang<sup>2</sup>

<sup>1</sup>Boston College, Institute for Scientific Research  
885 Centre St., Newton, MA 02459, United States

<sup>2</sup>Air Force Research Laboratory  
3550 Aberdeen Avenue SE, Kirtland AFB, NM 87117, United States

Corresponding Author: rezy.pradipta@bc.edu

## ABSTRACT

We report our investigation on the detection and classification of equatorial plasma bubble (EPB) structures in the Global-scale Observations of the Limb and Disk (GOLD) far ultraviolet (FUV) data. We have developed a novel technique for detrending the nighttime GOLD FUV irradiance data, which helps reveal large-scale field-aligned depletions associated with EPBs. The data detrending technique is a two-dimensional generalization of the rolling-barrel data detrending technique [Pradipta *et al.*, 2015] that operates in one dimension. In this case, the rolling barrel is replaced with a rolling ball with two degrees of freedom to navigate across a two-dimensional uneven terrain defined by the nighttime GOLD FUV irradiance data. The inferred baseline irradiance and the detrended irradiance data are subsequently transformed into geomagnetic coordinate in order to trace the position of the equatorial ionization anomaly (EIA) crests and the shape of EPB depletions. In the data analysis, the detected EPB depletions may appear either straight or curved with an inverse-C shape, depending on the solar local time. Zonal drift velocities of the detected EPBs are deduced based on sequential frames of GOLD FUV observation data. Afterwards, the computed EIA and EPB traces are transformed back from geomagnetic into geographic coordinate for realistic comparison with the original GOLD FUV observation data.

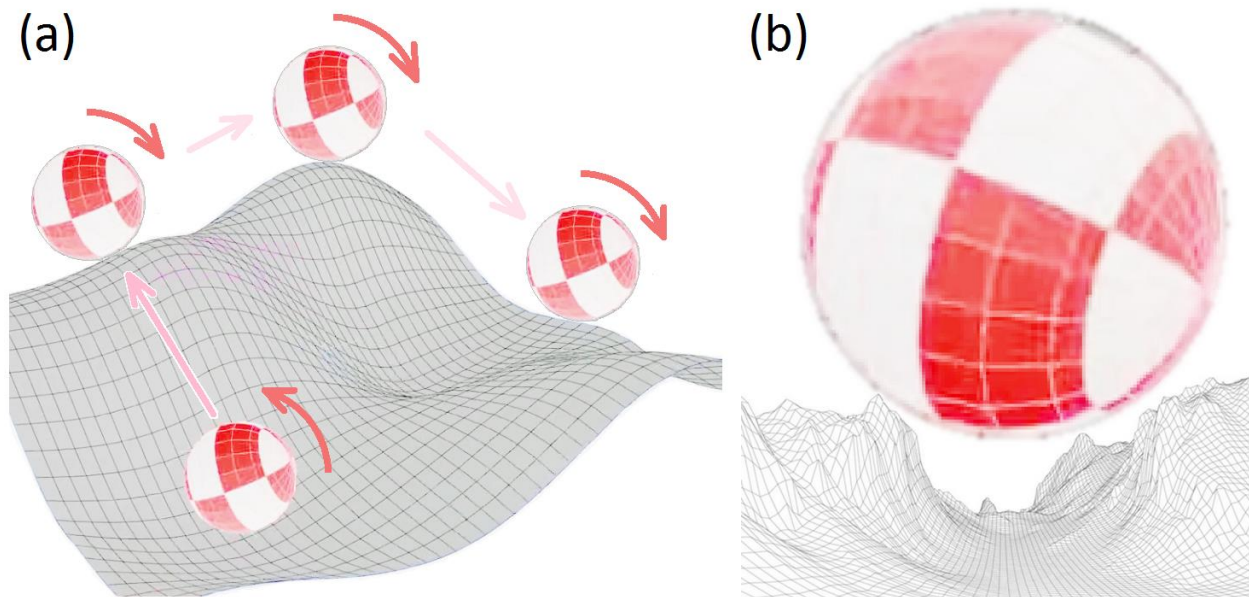
## 1. INTRODUCTION

Equatorial plasma bubbles (EPBs) are important space plasma phenomena in the nighttime low-latitude ionosphere due to their potential capacity to disrupt radio signals from navigation and communication satellites. Optical diagnostics of airglow emissions from the upper atmosphere can be used for monitoring and detecting EPBs, which often appear in the observation data as dark, bifurcating bands. Aforementioned optical observations of EPBs can be carried out either using ground-based all-sky imagers or using space-borne imaging instruments. Launched in 2018, the Global-scale Observations of the Limb and Disk (GOLD) mission contains such a space-borne imaging spectrograph that can be utilized for EPB observations over the Atlantic longitude sector.

Given the highly inhomogeneous configuration of the low-latitude ionosphere, particularly due to the equatorial ionization anomaly (EIA) crests at approximately  $\pm 15$  deg MLAT, data detrending is sometimes necessary in order to reveal the detailed structures of the EPB plumes. However,

the fact that EPBs manifest themselves in the data as deep negative excursions or depletions (instead of zero-average wave fluctuations) poses some challenge in performing the detrending. A special data detrending technique for extracting EPB profiles from GPS total electron content (TEC) observations was proposed by *Pradipta et al.* [2015]. This technique treats the GPS TEC signals as a form of terrain for a barrel to roll over the depletions, which allows us to correctly deduce the baseline TEC level as if the EPBs were absent. The baseline TEC level can then be used to calculate the net  $\Delta\text{TEC}$  values and reveal the EPB profiles.

Although quite effective in extracting EPB profiles from GPS TEC observations, the above data detrending technique works only in 1-dimensional context of TEC signals from individual GPS satellite passes. In the case of detrending the GOLD FUV data, an analogous 2-dimensional data detrending technique is desired. The present work aims to formulate such a 2-D data detrending technique for GOLD FUV observations, which would facilitate EPB identifications in the data.



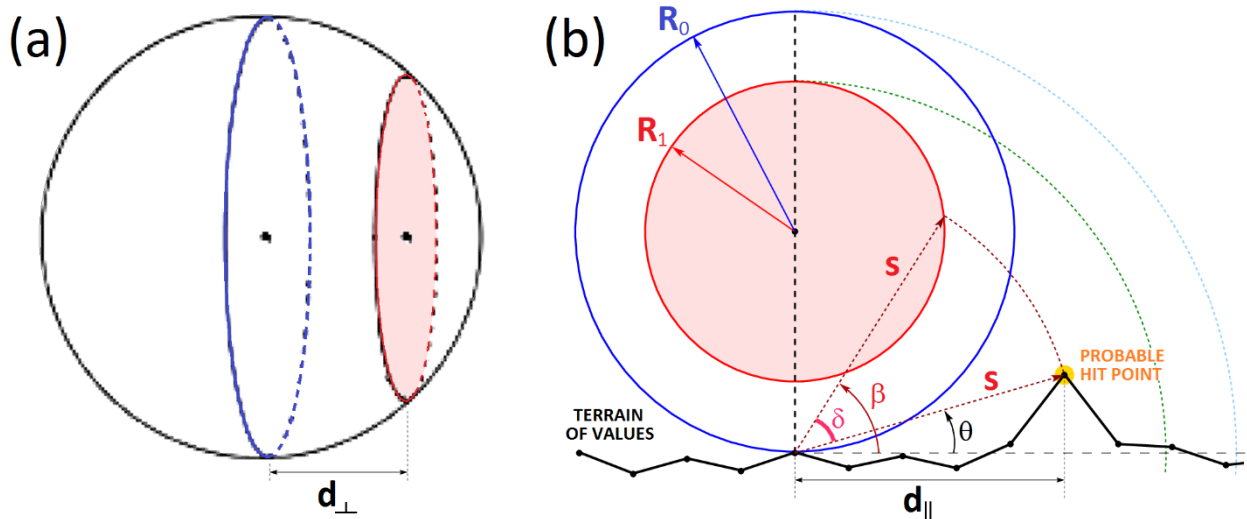
**Figure 1.** A graphical illustration of the rolling-ball data detrending process. (a) General navigation of the rolling ball on an uneven terrain. (b) A ball with sufficiently large radius should be able to skip/roll over narrow canyons/valleys – which would correspond to EPB depletions in the case of GOLD FUV data.

Figure 1 illustrates the 2-D data detrending technique that we are formulating, where we replace the rolling barrel with a rolling ball. The terrain on which the ball rolls would have come from the GOLD FUV observation data. In the following sections below we present the details.

## 2. DATA AND METHODOLOGY

In this work, we used the 135.6 nm nighttime emission data from the NASA GOLD mission. More specifically, we used the Level-1C data. The observation data files can be retrieved from either <https://gold.cs.ucf.edu/data> or <https://spdf.gsfc.nasa.gov/pub/data/gold/level1c>. In the analysis, observation data from the Channels A and B were joined together to obtain the full spatial coverage of nighttime FUV emission within the GOLD's field-of-view (FOV).

In this data detrending procedure, the GOLD FUV radiance  $\mathcal{R}$  (in Rayleighs, R) as a function of latitude  $\Lambda$  and longitude  $\Phi$  is first transformed via variable scaling. In particular, we apply the following set of transformations:  $X = \text{longitude}/\Phi_0$ ;  $Y = \text{latitude}/\Lambda_0$ ; and  $Z = \log_{10}[(\mathcal{R}+g_0)/G_0]$ . The most suitable scaling factors (determined by trial-and-error) for this purpose were  $\Phi_0 = 12^\circ$ ,  $\Lambda_0 = 5^\circ$ ,  $g_0 = 600 \text{ R} + \min(\mathcal{R})$ , and  $G_0 = 0.3 \text{ R}$ . In the XYZ-space, the radius of the rolling ball is  $R_0 = 1$  by default. This transformation compresses the dynamic range of the radiance values, and gives us a controlled way to select the effective size of the rolling ball relative to the terrain.



**Figure 2.** Basic mechanics for determining the next contact point of a rolling ball. (a) General distinction between the central wheel and off-center wheel of the rolling ball. (b) Geometry of a candidate for the next contact point relative to the corresponding off-center wheel.

Figure 2 illustrates the basic mechanics that controls how the ball rolls on the terrain. At each step, the main question is to determine which point on the terrain is going to be the next contact point of the ball. This is done by considering a subset of grid points on the terrain within the immediate “forward shadow” of the rolling ball. For each point within this area, we determine the corresponding off-center wheel that could hit the said point as the ball rolls forward, and compute the angle  $\delta = \beta - \theta$  as depicted in the diagram. The point with the smallest  $\delta$ -angle will be the next contact point.

Using this basic mechanics, we roll the ball around to cover the entire terrain in  $XY$ -space and mark the contact points. We then take the radiance values at the contact points and interpolate them onto the entire terrain grid. This interpolation establishes the baseline radiance level without the EPBs. Subtracting this baseline from the original data will give us the net radiance values.

### 3. RESULTS

Figure 3 shows a working example of the data detrending process. Figure 3a shows the original GOLD FUV radiance data (in geographic lat/lon coordinate) from observations on 2 February 2022 at 21:40 UTC. A number of EPB-related depletions are already visible in the data. Figure 3b shows the rastering process by the rolling ball (in the  $XY$ -space). The magenta dots mark the

contact points of the rolling ball as it traveled around the terrain. Figure 3c depicts the baseline radiance level that resulted from interpolating the radiance values at the contact points onto the whole grid (now back in geographic lat/lon coordinate). A bilinear numerical interpolation was used. Finally, Figure 3d shows the net radiance that we obtained by subtracting the baseline level from the original radiance data (in lat/lon coordinate). In the net radiance data, there is a significantly clearer contrast between unperturbed regions and the EPB-related depletions. Other things being equal, this enhanced contrast should lower the difficulty for EPB detection to some degree, compared to when working with the original GOLD FUV radiance data.

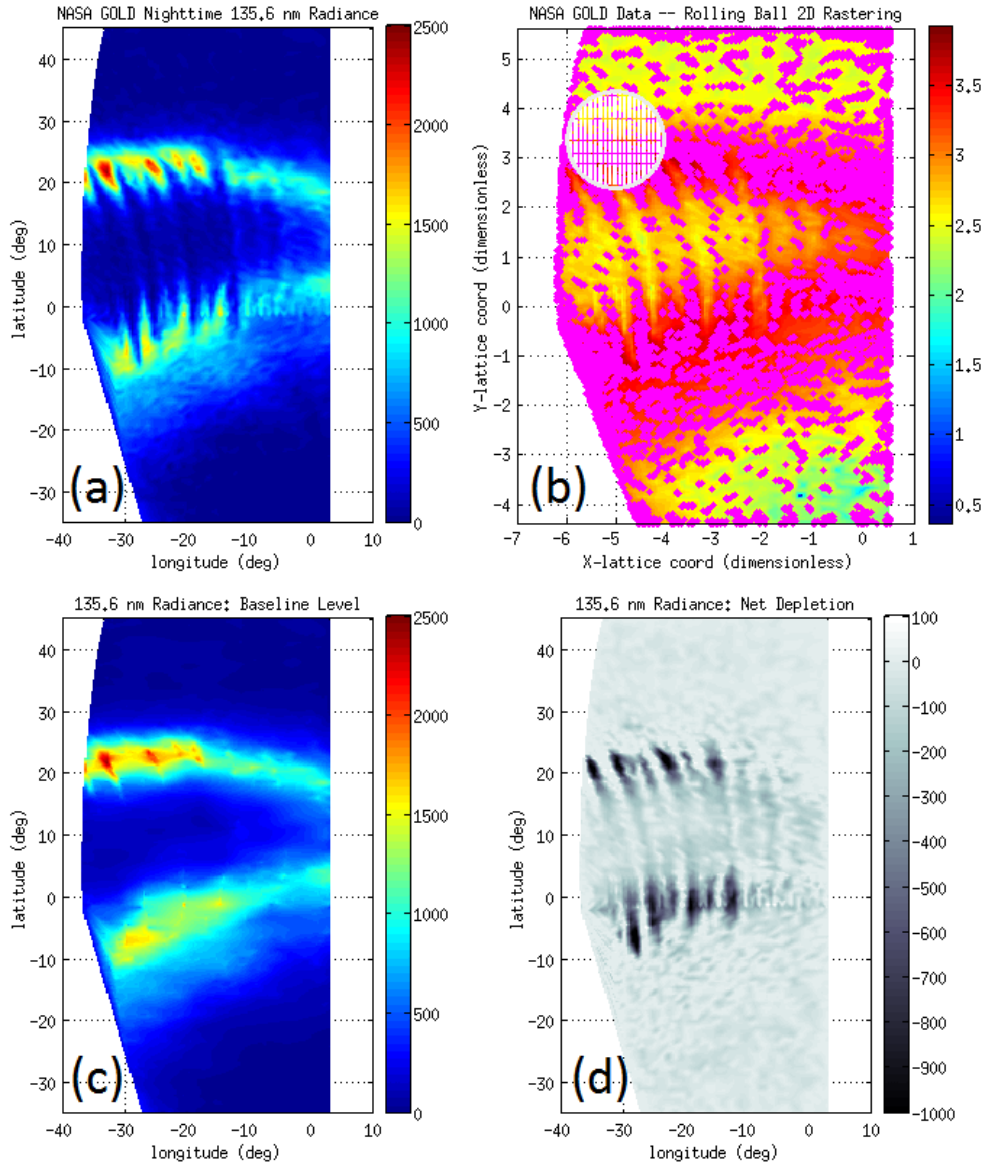


Figure 3. Step-by-step working illustration of the data detrending procedure. (a) Original GOLD radiance data. (b) Rastering process by the rolling ball. (c) Baseline level obtained by interpolating radiance values at the contact points. (d) Net radiance values obtained by subtracting the baseline from the original data.

To further facilitate the EPB detection, we can transform the net radiance data from geographic coordinate into geomagnetic latitude representation. This coordinate transformation should

remove the systematic tilt angle associated with the geomagnetic declination, thus making the depletion structures (dark bands) appear more upright. Further, the EPB depletions would also be more symmetrical, almost evenly split around the  $MLAT = 0^\circ$  line. Although it would not be perfect, these two factors should confer additional advantage to us for EPB detection.

Figure 4a shows the net radiance as a function of geographic longitude (at the magnetic equator line) and geomagnetic latitude. Figure 4b shows the same data after some additional smoothing, on which we superposed the numerically traced spines of the EPB depletions. The spines of the EPB depletions were traced inward starting from the two outer ends (at roughly  $\pm 15^\circ$  where the deepest depletions can be found), moving toward the  $0^\circ$  MLAT center point – akin to trekking along a narrow canyon. Here, 8 (eight) distinct EPB spines were detected by this procedure.

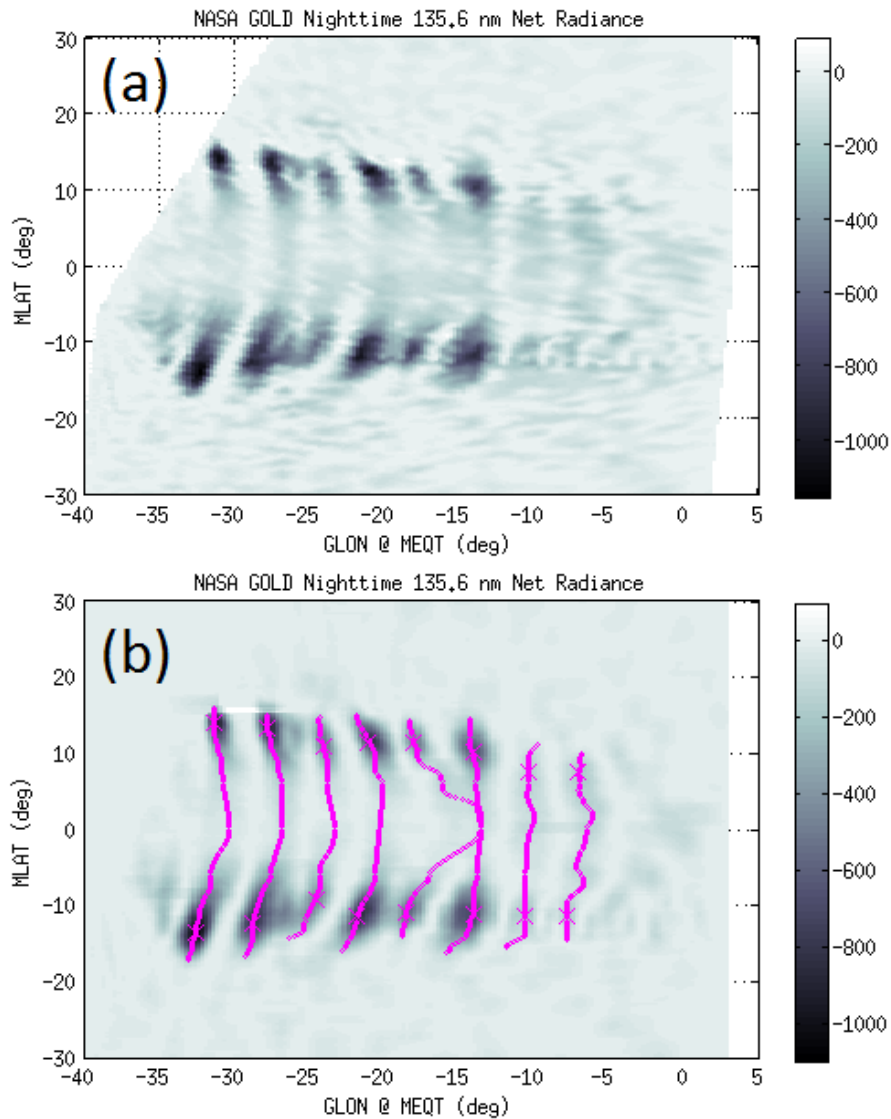


Figure 4. (a) Detrended GOLD FUV radiance data transformed into geomagnetic latitude representation, and (b) the same data plot overlaid with a set of arcs that correspond to the spines of EPBs recognized in the detrended GOLD FUV data.

The morphology of the EPB depletions found in Figure 4 shows an inverse-C shape, which is indicative of a sheared eastward zonal drift of the EPB plumes throughout the nighttime hours. One of the EPB plumes (number 5 from the left) shows an extreme bending, even touching its neighbor to the east. An examination of sequential frames of the GOLD FUV observation data on the same night, analyzed using identical computational procedure, confirmed the sheared EPB zonal drift velocity pattern mentioned above.

If needed, the numerically traced EPB spines may also be subsequently fitted using an analytical function, which would produce smoother arc shapes. Based on our testing thus far, symmetrical (even) functions including parabola, hyperbola, and  $\tan^4 x$  (i.e. tangent raised to fourth power) appear to be reasonable choice for this optional curve-fitting procedure.

#### **4. CONCLUSIONS**

In this work, we have formulated a 2-D data detrending technique to reveal EPB structures that are present in GOLD FUV observations. Analogous to rolling-barrel GPS TEC data detrending technique in 1-D, this new 2-D data detrending technique utilizes the mechanics of a rolling ball on uneven terrain. We demonstrated the working functionality of this data detrending procedure using test data from 2 February 2022 observations. The detrended net radiance data showed a sharper contrast between ambient regions and the EPB depletion regions, in comparison to the original GOLD FUV observation data. The better contrast in the net radiance data facilitate the process of tracing the spines of the EPB depletions numerically. Future works will continue in terms of improving the general reliability of the EPB detection and spine-tracing procedures, and exploring possibilities of practical applications afforded by this data detrending technique.

#### **ACKNOWLEDGEMENTS**

This work was supported by the NASA GOLD-ICON Guest Investigators (GIGI) program under grant #NNH22OB17A.

#### **REFERENCES**

Pradipta, R., Valladares, C. E., and Doherty, P. H. (2015), An effective TEC data detrending method for the study of equatorial plasma bubbles and traveling ionospheric disturbances, *J. Geophys. Res. Space Physics*, 120, 11,048–11,055, <https://doi.org/10.1002/2015JA021723>